Optica Applicata, Vol. XLIII, No. 3, 2013
DOI: 10.5277/oa130313

Theory of evanescent Bessel beams with a metallic sheet

SAUD AL-AWFI

Department of Physics, Taibah University, Medina, Saudi Arabia;
e-mail: alawfi99@hotmail.com

We explain how a surface optical vortex can be created when a Bessel beam is totally reflected internally at the planar surface of a dielectric on which a metallic sheet has been deposited. A two-dimensional patterning on the surface, the strongly localized intensity distribution decays with distance vertical to the surface. The characteristics of this surface optical vortex depend on the incident beam parameters and the dielectric mismatch of the media.

Keywords: optical vortex, optical lattice, metallic sheet, surface modes.

1. Introduction

It is well established that laser light prepared as a Bessel beam shows little diffraction, typically exhibiting a number of concentric high intensity rings separated by dark rings [1–4]. In particular, the central peak is considered to be remarkably stable against diffraction and it is this property that is behind the recent applications including atom guides, nonlinear optics and optical atom sorting [3].

We point out here that the non-diffractive feature also makes these beams suitable for the production of a surface optical vortex in which typically a Bessel beam propagating within an optically dense medium is totally internally reflected at a planar interface with vacuum. A light field possessing the rotational features of the Bessel beam, but which is tightly bound to the surface as an evanescent mode, is generated in the vacuum region, with its intensity in vacuum depending on the Bessel order and displaying interesting spatial variations while still decaying exponentially with distance away from the surface [5]. It was well-known that the diameter of the central lobe of the evanescent Bessel beams could be decreased to a value of a submicron order which gives rise to the opportunity of using evanescent Bessel beams in optical microscopy [6]. A further detailed theory of evanescent Bessel beams is given in Refs. [7–10].

The ultimate goal of the present work is to determine the action related to the surface mode due to a totally internally reflected Bessel beam and its optical angular momentum content whose origin is neither photon spin nor surface morphology, the required phase properties principally being conferred by a helical beam structure. As well as,

the work explores the possible applications that we can experimentally realize for systems in the vicinity of the surface.

The paper is organized as follows. In Section 2, we outline the field of Bessel light beams propagated within a non-dispersive medium. In Section 3, we describe the fundamental components of the physical model that is employed to produce surface modes, including a metallic sheet deposited on glass. The process needed for the requirement of the light mode bearing the evanescent part is then fully described, leading to suitable field distributions in structure regions. In Section 4, we briefly derive an expression for the total optical forces associated with an evanescent beam at the outer metallic sheet surface. We explain when this product of the optical forces profiles leads clearly to the presentation of a two-dimensional surface optical vortex. In Section 5, we provide comments and conclusion.

2. Bessel light beams

Consider the electric field of a Bessel beam travelling along a z-direction in a medium of constant refractive index n, characterized by the integer ℓ, angular frequency ω, and axial wavevector $k = nk_0$, where $k_0 = \omega/c$ is the wavevector in a vacuum. Such a beam with the plane polarized along the field vector can be written in cylindrical coordinates as [11]

$$\mathbf{E}^{I}_{k\ell}(\mathbf{r}, t) = \hat{\mathbf{y}}\mathbf{F}_{k\ell}(r_{||}, z)\exp\Big[i(kz - \omega t)\Big]\exp(i\ell\varphi) \tag{1}$$

where $F_{k\ell}(r_{||}, z)$ is the standard envelope function

$$\mathbf{F}_{k\ell}(r_{||}, z) = \eta_{k0}\sqrt{2\pi k_r w_0}\left(\frac{z}{z_{\max}}\right)^{\ell+1/2}\exp\left(-\frac{z^2}{z^2_{\max}}\right)\times \tag{2}$$

$$\times\exp\left[i\left(\ell\hat{\varphi} - \frac{\pi(2\ell-1)}{4}\right)\right]J_\ell(k_r r_{||})$$

where w_0 is the input beam waist, k_r is the radial wavevector and φ is the azimuthal coordinate. The factor η_{k0} is the amplitude of a corresponding plane wave of intensity I propagating in the dielectric medium of refractive index n

$$\eta_{k0} = \sqrt{\frac{2I}{n^2\varepsilon_0 c}} \tag{3}$$

while $z_{\max}$ is the typical ring spacing. The last term $J_\ell(k_r r_{||})$ is the Bessel function of the order ℓ. The mathematical formula of the Bessel beam that is given in Eq. (2) is only valid for the central region of the Bessel beam that has been produced. The main condition for this validity is $2w(z)/w_0 \approx 1$, where $w(z) = 1/k_r$ is a measure of the width of the central lobe in a J_0 beam or the central dark fringe in a higher-order beam which can be called the beam size at axial coordinate z. This can be written as

$$w(z) = w_0 \sqrt{1 + \left(\frac{\lambda z}{\pi w_0^2} \right)^2} \tag{4}$$

The plane $z = 0$ corresponds to the minimum beam waist $w(0) = w_0$ and on this plane the phase in Eq. (2) vanishes.

3. Physical model

The fundamental components of the physical model are shown in Fig. 1. Here a metallic sheet is deposited on a planar surface of a glass prism (forming the dielectric substrate). A Bessel beam of a given order ℓ and frequency ω is incident at an angle ϕ and is propagating on the left-hand side of the vertical axis within the glass prism. This beam is internally reflected at the inner interface between the prism and the metallic sheet, and partially leaks into the metallic sheet. The beam within the metallic sheet subsequently generates an evanescent mode in the vacuum region of the sheet system. A neutral atom possessing a transition frequency $\omega_0 < \omega$ moving in the plane of incidence towards the outer surface of the structure would be subject to an average repulsive dipole force plus an average light pressure force, both owing their existence to the presence of the evanescent field. The atom would also be subject to an average dipole image force. It is the combined influence of these average forces that can be made to control the vortex process.

It is easy to see that the relevant quantized electric field vector at the frequency ω can be written in terms of incident (I), reflected (R) and evanescent (evan) parts as follows [12]

$$E(\mathbf{k}_{||}, \mathbf{r}, t) = \left\{ \left[\mathbf{F}^I(\mathbf{r}) + \mathbf{F}^R(\mathbf{r}) \right] \Theta(-z) + \mathbf{F}^{\text{evan}}(\mathbf{r}) \Theta(-z) \right\} \exp\left[i(\mathbf{k}_{||} \cdot \mathbf{r}_{||} - \omega t) a \right] + \text{H.c.} \tag{5}$$

where a is a mode annihilation operator, H.c. stands for the Hermitian conjugate, and Θ is the unit step function. The three standard envelope functions $\mathbf{F}(\mathbf{r})$ are given by

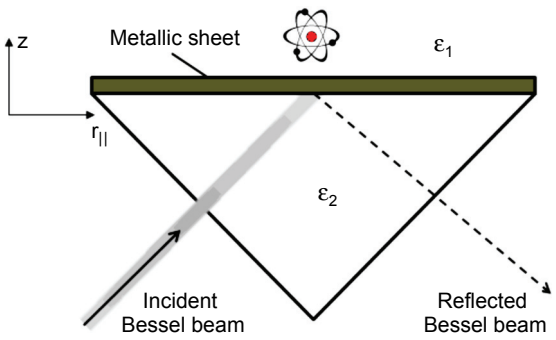

Fig. 1. Schematic illustration of the physical model.

$$\mathbf{F}^{I}(\mathbf{r}) = A^{I}\left(1,\, 0,\, -\frac{k_{||}}{k_{z2}}\right)\exp(ik_{z2}z) \tag{6}$$

$$\mathbf{F}^{R}(\mathbf{r}) = A^{R}\left(1,\, 0,\, \frac{k_{||}}{k_{z2}}\right)\exp(ik_{z2}z) \tag{7}$$

$$\mathbf{F}^{\text{evan}}(\mathbf{r}) = B\left(1,\, 0,\, \frac{ik_{||}}{k_{z1}}\right)\exp(-k_{z1}z) \tag{8}$$

Here $\mathbf{k}_{||}$ is the wavevector parallel to the surface. Its magnitude $k_{||}$ is given by $c^2k_{||}^2 = = \omega^2\varepsilon_2\sin^2(\phi)$ where ϕ is the angle of incidence. The three quantities between the brackets in Eqs. (6) to (8) stand for the vector components parallel to $\mathbf{k}_{||}$, vertical to it on the surface plane and along the z-direction, respectively. k_{z1} and k_{z2} (both real) are defined by

$$k_{z1}^2 = k_{||}^2 - \frac{\varepsilon_1\omega^2}{c^2} > 0 \tag{9}$$

$$k_{z2}^2 = \frac{\varepsilon_2\omega^2}{c^2} - k_{||}^2 > 0 \tag{10}$$

Finally, A^I, A^R and B are the field amplitude factors to be determined. The notation is such that the parameters associated with the substrate are labelled by the subscript 2, while for the outer region (the vacuum) the label is 1. The dielectric function ε_2 is assumed, in general, to be frequency-dependent while we assume that $\varepsilon_1 \equiv \varepsilon_0 = 1$, as appropriate for a vacuum. The role of the metallic sheet is primarily to provide a two-dimensional charge density n_s and so, an electric conductivity $in_se^2/m^*(\omega + i\gamma)$, where m^* and e are the electronic effective mass and charge, respectively, and $\gamma \ll \omega$ accounts for film plasma loss effects. The metallic sheet only enters the formalism via the electromagnetic boundary conditions involving the tangential components of the magnetic fields corresponding to Eqs. (6) to (8). This can be calculated using Maxwell's equation $\mathbf{H} = -(i\varepsilon_0c^2/\omega)\nabla\times\mathbf{E}$. The application of the first boundary condition, namely the continuity of the tangential component of the electric field vector at $z = 0$, yields

$$A^I + A^R = B \tag{11}$$

The second electromagnetic boundary condition is that the tangential component of the magnetic field vector experiences a discontinuity at $z = 0$, arising from the surface current induced by the in-plane component of the electric field at the metallic sheet. We have

$$H_{||}(0_-) - H_{||}(0_+) = \frac{in_se^2}{m^*(\omega + i\gamma)}E_{||}(0) \tag{12}$$

where $0_{\pm}$ are the limit as $\zeta \to 0$ of $(0 \pm \zeta)$. Application of the boundary condition leads to a second relation connecting the field amplitudes

$$\frac{\varepsilon_2}{k_{z2}}(A^I - A^R) + \frac{i\varepsilon_1}{k_{z1}}B = \frac{in_s e^2}{\varepsilon_0 m^* \omega(\omega + i\gamma)} \tag{13}$$

Elimination of A^R between Eqs. (11) and (13) yields straightforwardly

$$B = 2A^I \left[\frac{ik_{z2}}{\varepsilon_2} \left(\frac{n_s e^2}{\varepsilon_0 m^* \omega(\omega + i\gamma)} - \frac{\varepsilon_1}{k_{z1}} \right) + 1 \right]^{-1} \tag{14}$$

The amplitude A^I of the incident field is conveniently fixed by canonical methods, treating the incident field as though it is in an infinite bulk. The field Hamiltonian H^I is such that

$$H^I = \frac{\varepsilon_0}{2} \int \mathrm{d}\mathbf{r} \left[\frac{\partial(\omega\varepsilon_2)}{\partial\omega}(E^I)^2 + \frac{1}{\varepsilon_0 c}(B^I)^2 \right] =$$

$$= \frac{1}{2}\hbar\omega \left[a(\mathbf{k}_{||})a^{\dagger}(\mathbf{k}_{||}) + a^{\dagger}(\mathbf{k}_{||})a(\mathbf{k}_{||}) \right] \tag{15}$$

where the label I emphasizes the incident part of the electric field in the substrate with H^I the corresponding magnetic field. The canonical condition equation (15) gives straightforwardly

$$A^I = \frac{\sqrt{2\pi}\,\eta_{k0}}{\left[1 + (\lambda z/\pi w_0^2)^2\right]^{1/4}} \left(\frac{z}{z_{\max}} \right)^{\ell + 1/2} \exp\left(-\frac{z^2}{z_{\max}^2} \right) \times$$

$$\times \exp\left\{ i \left[\ell \tan^{-1}\left(\frac{y}{x} \right) - \frac{\pi(2\ell - 1)}{4} \right] \right\} J_{\ell} \left(\frac{r_{||}}{w_0 \sqrt{1 + (\lambda z/\pi w_0^2)^2}} \right) \tag{16}$$

Thus in the view of Eqs. (5), (8) and (14), the evanescent electric will be given as

$$\mathbf{E}^{\mathrm{evan}}(\mathbf{r}, t) = \frac{2A^I \left(1, 0, i\dfrac{k_{||}}{k_{z1}} \right) \exp(-k_{z1}z)}{\dfrac{ik_{z2}}{\varepsilon_2} \left(\dfrac{n_s e^2}{\varepsilon_0 m^* \omega(\omega + i\gamma)} - \dfrac{\varepsilon_1}{k_{z1}} \right) + 1} \times$$

$$\times \exp\left[\frac{-ix\sqrt{\varepsilon_2}\,\omega\sin(\phi)}{c} \right] \exp(i\omega t) \tag{17}$$

Using the continuity formalism as in [13, 14] of the electric field vector tangential to the surface, along with exponential decay with the coordinate z, the structure of the Bessel evanescent field $\mathbf{E}_B^{\text{evan}}$ in the vacuum region can be given as

$$\mathbf{E}_B^{\text{evan}}(\mathbf{r}) = \mathbf{E}^{\text{evan}}\Big(x \to x\cos(\phi), y, z \to -x\sin(\phi)\Big) \tag{18}$$

4. Manipulating optical forces

The total steady state force acting on the centre of mass of an atom moving near the metallic sheet surface of transition frequency ω_0 moving in the vacuum region at velocity vector $\mathbf{V}(t) = \dot{\mathbf{r}}(t)$ is given by the well-known expression [15, 16]

$$\mathbf{F}(\mathbf{r}, \mathbf{V}) = 2\hbar\left\{\frac{\Gamma(\mathbf{r})\Omega^2(\mathbf{r})\nabla\theta(\mathbf{r}) - \frac{1}{2}\Delta(\mathbf{r}, \mathbf{V})\nabla\Omega^2(\mathbf{r})}{\Delta^2(\mathbf{r}, \mathbf{V}) + \Omega^2(\mathbf{r}) + \Gamma^2(\mathbf{r})}\right\} \tag{19}$$

where $\Gamma(\mathbf{r})$ is the decay emission rate of the atom, $\Omega(\mathbf{r})$ is the Rabi frequency for an electric dipole $\boldsymbol{\mu}$ approaching the surface from the vacuum region ($z > 0$) and, so interacting with the evanescent light. The Rabi frequency is defined as [12]

$$\Omega(z \geq 0) = \left|\frac{\boldsymbol{\mu} \cdot \mathbf{E}_B^{\text{evan}}(\mathbf{r})}{\hbar}\right| \tag{20}$$

$\theta(\mathbf{r})$ represents the evanescent light phase which corresponds to the momentum imparted by the evanescent light to the atom and, in view of Eqs. (2) and (17), can be written as

$$\theta(x, y) = \left[\ell\tan^{-1}\left(\frac{y}{x\cos(\phi)}\right) - \frac{\pi(2\ell - 1)}{4}\right] - \frac{\sqrt{\varepsilon_2}\, x\omega\sin(\phi)}{c} \tag{21}$$

Thus $\theta(x, y)$ has the gradient

$$\nabla\theta(x, y) = \alpha(x, y)\hat{\mathbf{x}} + \beta(x, y)\hat{\mathbf{y}} \tag{22}$$

where

$$\alpha = \frac{-\ell y}{x^2\cos(\phi)\left[1 + \left(\frac{y}{x\cos(\phi)}\right)^2\right]} - \frac{\sqrt{\varepsilon_2}\,\omega\sin(\phi)}{c} \tag{23}$$

$$\beta = \frac{\ell}{x\cos(\phi)\left[1 + \left(\frac{y}{x\cos(\phi)}\right)^2\right]} \tag{24}$$

Finally, $\Delta(\mathbf{r}, \mathbf{V})$ is the dynamic detuning given by

$$\Delta = \Delta_0 - \mathbf{V} \cdot \nabla\theta \tag{25}$$

where $\Delta_0 = (\omega - \omega_0)$ is the static detuning of the light from the atomic resonance. Another expression where the phase gradient enters is the first term of the force field given in Eq. (19). Substituting for $\nabla\theta$ from Eq. (22), the first term of the force field (the dissipative force $\mathbf{F}_{\text{diss}}$) can be written as

$$\mathbf{F}_{\text{diss}}(\mathbf{r}, \mathbf{V}) = \left\{\frac{2\hbar\alpha\Gamma(\mathbf{r})\Omega^2(\mathbf{r})}{\Delta^2(\mathbf{r}, \mathbf{V}) + \Omega^2(\mathbf{r}) + \Gamma^2(\mathbf{r})}\right\}\hat{\mathbf{x}} + \left\{\frac{2\hbar\beta\Gamma(\mathbf{r})\Omega^2(\mathbf{r})}{\Delta^2(\mathbf{r}, \mathbf{V}) + \Omega^2(\mathbf{r}) + \Gamma^2(\mathbf{r})}\right\}\hat{\mathbf{y}} \tag{26}$$

The dissipative force has been exploited in heating and cooling the atomic motion. As Equation (26) suggests, to influence the atom in x–y directions, the integer ℓ must be greater than zero, otherwise the atom will only be subject to a force in x-direction. In this case, the dissipative force reduces to

$$\mathbf{F}_{\text{diss}}(\mathbf{r}, \mathbf{V}) = 2\hbar\left\{\frac{\Gamma(\mathbf{r})\Omega^2(\mathbf{r})\left(\frac{-\sqrt{\varepsilon_2}\,\omega\sin(\phi)}{c}\right)}{\Delta^2(\mathbf{r}, \mathbf{V}) + \Omega^2(\mathbf{r}) + \Gamma^2(\mathbf{r})}\right\} \tag{27}$$

On the other hand, the second term of the force field of the dipole force $\mathbf{F}_{\text{dip}}$ given in Eq. (19) which is used for trapping and can be written as

$$\mathbf{F}_{\text{dip}}(\mathbf{r}, \mathbf{V}) = \hbar\left\{\frac{\Delta(\mathbf{r}, \mathbf{V})\nabla\Omega^2(\mathbf{r})}{\Delta^2(\mathbf{r}, \mathbf{V}) + \Omega^2(\mathbf{r}) + \Gamma^2(\mathbf{r})}\right\} \tag{28}$$

This means that the atoms also become subject to a light induced dipole force and this, too, depends on the order of the mode. The explicit form of the dipole potential for such mode is such that $F_{\text{dip}} = -\nabla U$, with U in this case written as

$$U(\mathbf{r}, \mathbf{V}) = \frac{\hbar\Delta(\mathbf{r}, \mathbf{V})}{2}\ln\left(1 + \frac{2\Omega^2(\mathbf{r})}{\Delta^2(\mathbf{r}, \mathbf{V}) + \Gamma^2(\mathbf{r})}\right) \tag{29}$$

4.1. Surface optical lattice ($\ell = 0$)

To show the effects of the evanescent light on matter localized near the surface, we consider adsorbed sodium atoms that possess a transition frequency ω_0 such that ω_0 is at near-resonance with the frequency ω of the light. The evanescent field has significant intensity distribution in the vicinity and so the adsorbed atom will be subject to corresponding dissipative force $\mathbf{F}_{\text{diss}}$ and optical potential U that influence its

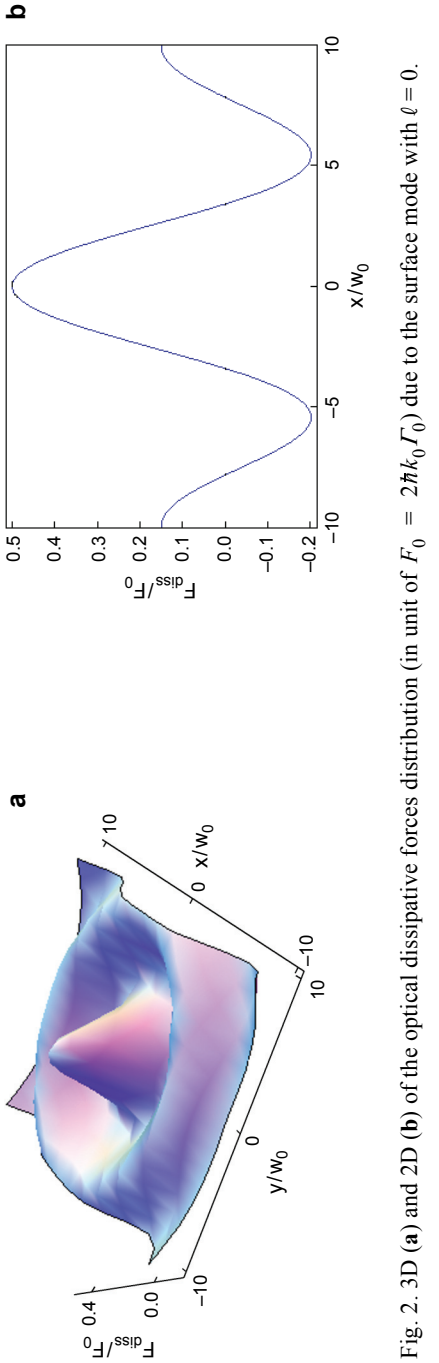

Fig. 2. 3D (**a**) and 2D (**b**) of the optical dissipative forces distribution (in unit of $F_0 = 2\hbar k_0 \Gamma_0$) due to the surface mode with $\ell = 0$.

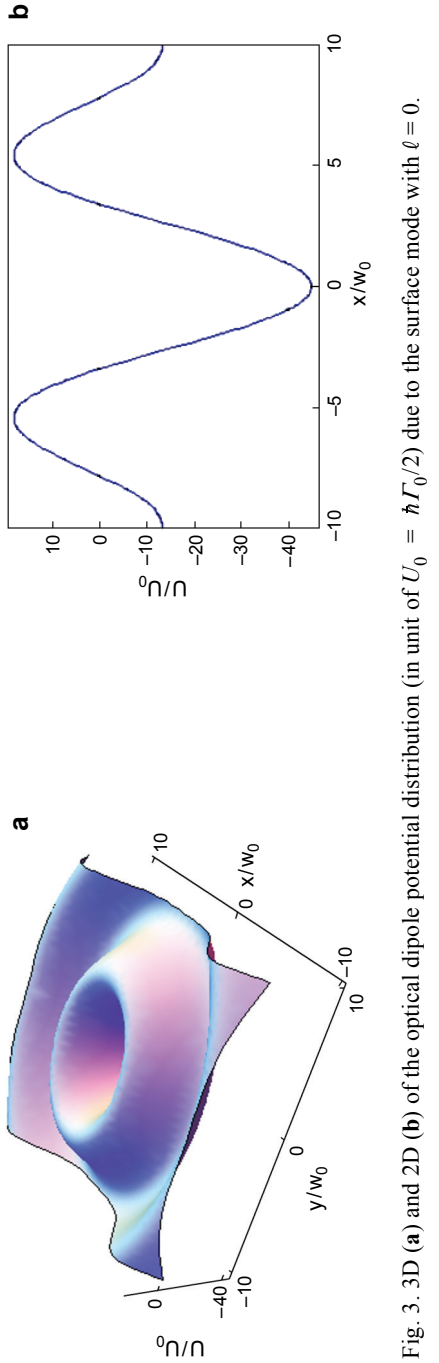

Fig. 3. 3D (**a**) and 2D (**b**) of the optical dipole potential distribution (in unit of $U_0 = \hbar\Gamma_0/2$) due to the surface mode with $\ell = 0$.

T a b l e 1. Parameters used for the illustration of the optical potential of sodium atoms in a surface metallic sheet deposited on glass.

$I = 2.0\times10^5$ Wm^{-2}	$V(0) = (0, 0)$	$\lambda_0 = 589$ nm	$\mu = 2.6a_B$
$\Gamma_0 = 6.1\times10^7$ s^{-1}	$\lvert\Delta_0\rvert = 5.0\times10^2\Gamma_0$	$\varepsilon_2 = 2.298$	$\phi = 42°$
$n_s^{\text{silver}} = 5.573\times10^{18}$ m^{-2}	$n_s = 215n_s^{\text{silver}}$	$w_0 = 40\lambda$	

in-plane motion. These distributions correspond to $\ell = 0$ and are shown in Figs. 2 and 3, respectively. They are plotted at a fixed value of $z > 0$ close to the metallic sheet surface for which the parameters are given in Table 1.

The produce dissipative force has different maxima and minima values that can be used to heat (or cool) atoms that have transition frequencies suitably detuned from the frequency ω of the light. The maximum value is located at the middle where $(x, y) = (0, 0)$ which means that atoms located at this point experience the strongest force along the axis. It can also be seen that the produce optical potential possesses distinct maxima and minima values that could be used to trap atoms that have transition frequencies suitably detuned from the frequency ω of the light. Additionally, it can be noted that the profile of the potential is actually not as an ideal back bowl-shaped quantum well, but has a slightly elliptical profile, because the light strikes the surface at the angle of incidence ϕ.

We can observe that the optical system with $\ell = 0$ formed a surface optical lattice, hence will attract any moving atom towards the surface [12–15]. As well, the depth of the quantum well can be controlled by varying the intensity and incident angle of the light. Finally, we can deduce from Fig. 3 that, from a quantum-mechanical point of view, solutions of the two-dimensional Schrödinger equation with U as potential must exist. In the ground state, the atomic wave function peaks in the vicinity of the central minimum associated with the dipole potential. It can be seen from Fig. 3 that for the parameters assumed above, the central well depth is approximately $(-45U_0)$. This is adequately deep to allow several quasi-harmonic trapping (vibrational) states. The vibrational frequency can be estimated simply using the parabolic approximation [17] while the precise details of the vibrational energy levels can be obtained straightforwardly by the numerical solution of the two-dimensional Schrödinger equation involving the full potential [18].

4.2. Surface optical vortex ($\ell \geq 0$)

The optical potential distribution corresponding to $\ell = 1$ is shown in Fig. 4, with the same parameters as shown in Table 1. It can be noted that the produce potential possesses different maxima and minima that can be used to trap atoms that have transition frequencies appropriately detuned from the frequency ω of the light. Similarly as in the previous case, with the same reason, the potential profile is not as an ideal annulus shaped quantum well, but is slightly elliptical.

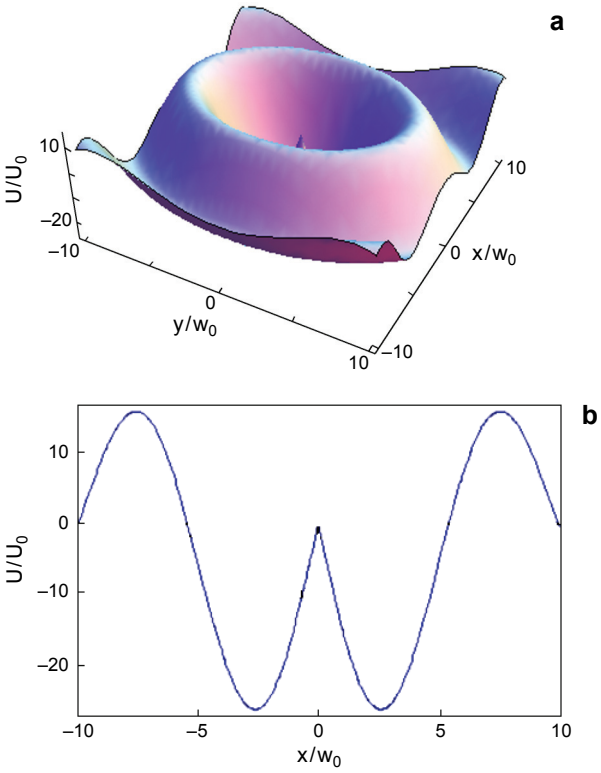

Fig. 4. 3D (**a**) and 2D (**b**) of the optical dipole potential distribution (in unit of $U_0 = \hbar\Gamma_0/2$) due to the surface mode with $\ell = 1$.

The combination of this potential with the two parts of the dissipative force associated with Eq. (27) will produce a more complex configuration that will give rise to additional effects in terms of atom dynamics which could not have been realized with $\ell = 0$. This is due to the orbital angular momentum property associated with the azimuthal dependence of light structure. The interaction process gives rise to a number of rotational effects which will make the atomic motion drastically different from that associated with $\ell = 0$. These rotational effects create the new phenomenon referred to as a surface optical vortex.

The dynamics of an atom of mass M immersed in the evanescent field follows straightforwardly by solving a Newtonian equation of motion, driven by a sum of the dissipative and dipole forces

$$M\frac{\mathrm{d}\mathbf{r}^2}{\mathrm{d}t^2} = \mathbf{F}_{\mathrm{diss}} + \mathbf{F}_{\mathrm{dip}} \tag{30}$$

We expect this solution directly leads to rotational motion as the signature of orbital angular momentum property mentioned above, leading to vibrational motion in a radial direction and resulting in an overall zigzag trajectory [13–15]. Clearly the optical

forces for any value of the parameter $\ell > 1$ can be obtained in a similar manner and controlling their values by varying mainly the light beam parameters and its angle of incident.

5. Conclusions

The main aim of the work discussed in the present paper serves to exemplify the physics associated with vortex characteristics in an evanescent electromagnetic field generated in vacuum, outside the metallic sheet surface of an optically dense dielectric medium. To show the mechanical influences of the associated optical forces, we have considered a neutral sodium atom immersed in the evanescent field, controlled by a surface optical vortex produced by the simplest Bessel beam vortex, the $\ell = 1$ mode.

Our study concerned especially an evanescent mode produced by laser light with an azimuthal phase dependence and orbital angular momentum as typified by Bessel beams. For such kind of light, the helical wavefront is corresponding to an optical vortex, consequently the evanescent fields produced by total internal reflection have vortex properties. We have explained how a single Bessel beam, totally internally reflected at the general interface of the metallic sheet and the medium within which the light is incident, produces a surface optical vortex in the vacuum region.

This is a theory that in principle applies to surface optical vortices produced by any order of Bessel modes and also to any optical mode characterized by an optical vortex. Between the possible applications, we can envisage the production of cautiously designed surface optical vortex arrays being used to create a pre-determined two-dimensional pattern for the manipulation and the surface deposition of atoms, a technique that has a possible relevance to the fields of nanolithography and other methods that involve the motion of atomic components localized near a surface. The theory is also willingly extendable to systems in which the evanescent mode couples into a fluid, rather than vacuum. For example, it is conceivable that the rotary motions of larger particles, trapped by optical tweezers near a fluid surface, may be afforded by such advances and are really attracting.

References

[1] Durnin J., Miceli J.J., Eberly J.H., *Diffraction-free beams*, Physical Review Letters **58**(15), 1987, pp. 1499–1501

[2] Durnin J., *Exact solution for nondiffractings beam. I. The scalar theory*, Journal of the Optical Society of America A **4**(4), 1987, pp. 651–654.

[3] McGloin D., Dholakia K., *Bessel beams: diffracting in new light*, Contemporary Physics **46**(1), 2005, pp. 15–28.

[4] McGloin D., Garces-Chavez V., Dholakia K., *Interfering Bessel beams for optical micromanipulation*, Optics Letters **28**(8), 2003, pp. 657–659.

[5] Ruschin S., Leizer A., *Evanescent Bessel beams*, Journal of the Optical Society of America A **15**(5), 1998, pp. 1139–1143.

[6] Grosjean T., Courjon D., Van Labeke D., *Bessel Beams as virtual tips for near-field optics*, Journal of Microscopy **210**(3), 2003, pp. 319–323.

[7] KURILKINA S.N., BELYI V.N., KAZAK N.S., *Features of evanescent Bessel light beams formed in structures containing a dielectric layer*, Optics Communications **283**(20), 2010, pp. 3860–3868.
[8] QIWEN ZHAN, *Evanescent Bessel beam generation via surface plasmon resonance excitation by a radially polarized beam*, Optics Letters **31**(11), 2006, pp. 1726–1728
[9] JIEFENG XI, QING LI, JIA WANG, *Numerical simulation of evanescent Bessel beams and apodization of evanescent field in near-field optical virtual probe*, Proceedings of SPIE **5635**, 2005, pp. 42–47.
[10] AL-MUHANNA M.K., KURILKINA S.N., BELYI V.N., KAZAK N.S., *Energy flow patterns in an optical field formed by a superposition of evanescent Bessel light beams*, Journal of Optics **13**(10), 2011, article 105703.
[11] AL-AWFI S., BOUGOUFFA S., *Generation of surface optical vortices by evanescent Bessel beams*, International Journal of Physical Sciences **7**(25), 2012, pp. 4043–4048.
[12] KIRK J., BENNETT C., BABIKER M., AL-AWFI S., *Atomic reflection of evanescent light in the presence of a metallic sheet*, Physics of Low-Dimensional Structures, No. 3/4, 2002, pp. 127–132.
[13] LEMBESSIS V.E., AL-AWFI S., BABIKER M., ANDREWS D.L., *Surface plasmon optical vortices and their influence on atoms*, Journal of Optics **13**(6), 2011, article 064002.
[14] ANDREWS D.L., BABIKER M., LEMBESSIS V.E., AL-AWFI S., *Surface plasmons with phase singularities and their effects on matter*, Physica Status Solidi – Rapid Research Letters **4**(10), 2010, pp. 241–243.
[15] ANDREWS D.L., BABIKER M., LEMBESSIS V.E., AL-AWFI S., *Optical vortex singularities and atomic circulation in evanescent waves*, Proceedings of SPIE **7950**, 2011, article 795007.
[16] AL-AWFI S., BABIKER M., LEMBESSIS V.E., ANDREWS D.L., *Generation of surface optical screw dislocations by evanescent plasmonic modes*, 2011 Saudi International Electronics, Communications and Photonics Conference (SIECPC), 2011, article 5877009.
[17] ALLEN L., BABIKER M., LAI W.K., LEMBESSIS V.E., *Atom dynamics in multiple Laguerre–Gaussian beams*, Physical Review A **54**(5), 1996, pp. 4259–4270.
[18] AL-AWFI S., *Schrödinger modal structure of sodium atom between parallel plates*, International Journal of Modern Physics B **18**(10–11), 2004, pp. 1515–1523.

Received May 4, 2012
in revised form November 18, 2012